

Numerical study of nugget formation in resistance spot welding

M.Hamedi, H.Pashazadeh

Abstract—Resistance spot welding is a widely used joining process for fabricating sheet metal assemblies in automobile industry. In comparison with other welding processes, RSW is fast and easy for automation. This process involves electrical, thermal and mechanical interactions. These make the whole welding procedure highly non-linear and difficult to model. This paper presents the modeling and simulation of spot welding, using finite element code, ANSYS. A two-dimensional axisymmetric model was used to simulate the thermo-electro-mechanical coupling of process. In order to improve accuracy, material properties were defined temperature-dependent and phase transformation was taken into account in simulation. Also thermal contact conductivity (TCC) and electrical contact conductivity (ECC) were considered temperature-dependant. Through simulation, thermal history of process and temperature distributions were predicted. Development of weld nugget during process and effect of process parameters on nugget formation were investigated.

Keywords—Finite element model, Resistance spot welding, Temperature distributions, Weld nugget

I. INTRODUCTION

RESISTANCE spot welding is a process of joining two or more metal sheets by fusion at discrete spots at the sheets interface. Resistance to current flow through the metal sheets generates heat. Temperature rises at the sheet interface till the plastic point of the metal is reached, the metal will begin to fuse and a nugget is formed. Current is then switched off and nugget is allowed to cool down slowly to solidify under pressure. This process is completed within a specified cycle time. The welding process was invented in 1877 by Professor Elihu Thomson and has been extensively used since then in the manufacturing industries for joining metal sheets [1]. The two main industries that widely use this process are the automobile industries and the aircraft industries.

The 3 main welding parameters are current, force and weld time. All these parameters need to be controlled effectively in order to produce a good weld quality. The spot welding process consists of 4 stages:

Squeeze cycle: time during which the upper electrode is

brought in contact with the sheets that need to be welded and force is exerted at the region that need to be welded.

Weld cycle: time during which current is turned on and resistance to current flow at the sheet interface produces a nugget.

Hold cycle: time during which the current is turned off and the fully grown nugget is allowed to cool slowly and solidify under constant pressure till it.

Off cycle: time during which the electrode is raised from the welded sheets and moved to the next welding location.

Some work has already been carried out on the modeling and simulation of a spot welding process. Cho et al. modeled electrical-thermal coupling of process [2]. Wei and Ho in their work modeled the spot welding process using numerical modeling [3]. They created an unsteady, axisymmetric heat conduction model to investigate 3-dimensional nugget growth for different welding current. Khan et al. used ABAQUS code to develop an axisymmetric finite element model employing coupled thermal-electrical-mechanical analysis [4]. Tsai et al. created a 2-dimensional axisymmetric model using ANSYS to do some parametric studies on the spot welding process [5]. Furthermore, more sophisticated FEM models which considered temperature dependent material properties, contact status, phase changing and coupled field effects into the simulation of resistance spot welding (RSW), have been developed [6-9].

In this paper a 2D axisymmetric model of finite element method was developed to simulate RSW process, using commercial software, ANSYS. Temperature distributions at different weld stages were obtained. Through temperature distributions weld nugget formation and its size were predicted. Also effects of welding current, welding time and electrode force on nugget formation were investigated.

II. THEORETICAL ANALYSIS

The governing equation for transient conduction in a two-dimensional cylindrical coordinate system with internal heat generation can be stated as [10]:

$$\frac{1}{r} \frac{\partial}{\partial r} \left(rK \frac{\partial T}{\partial r} \right) + \frac{1}{r} \frac{\partial}{\partial z} \left(rK \frac{\partial T}{\partial z} \right) + \dot{Q} = \rho c \frac{\partial T}{\partial t} \quad (1)$$

Where r and z are radial and axial coordinates and ρ , c , and K are density, specific heat, and thermal conductivity of the material respectively. The material properties are assumed

Manuscript received March 18, 2008; Revised received May 29, 2008

Hamed Pashazadeh is with Department of Mechanical Engineering, University of Tehran, Tehran, Iran (corresponding author to provide phone: +98-411-3803836; e-mail: hamed_pashazadeh@yahoo.com).

Mohsen Hamedi is with Department of Mechanical Engineering, University of Tehran, Tehran, Iran (e-mail: mhamedi@ut.ac.ir).

to be temperature dependant. The term \dot{Q} refers to the rate of the internal heat generation per unit volume within the boundary of the region of analysis. This particular term accounts for the Joule heating due to bulk resistivity in the sheet-electrode system.

It has been assumed that the boundary at the electrode edge in contact with the cooling water is maintained at uniform temperature. Thus, the boundary conditions to be implemented can be stated as follows:

$$T = T_{s1} \quad (2)$$

T_{s1} is temperature of the inner surface of electrode. On the outer surface of electrode the boundary condition is:

$$q = -K \frac{\partial T}{\partial n} = \alpha(T - T_o) \quad (3)$$

Where q , T_o , and α are the heat generation per unit volume, temperature of the surrounding air, and heat transfer constant. $\frac{\partial}{\partial n}$ is the gradient along the outward normal direction of the boundary.

Since only one-half of the sheet-sheet assembly has been considered for modeling because of the axial symmetry of the electrode geometry. This can be stated in the form that the radial heat transfer across the sheet and electrode symmetry line is zero, i.e.

$$\frac{\partial T}{\partial r} = 0 \quad (4)$$

III. NUMERICAL MODEL DEVELOPMENT

Fig. 1 shows the block diagram for the finite element computational procedure. The welding process starts with the squeeze cycle in which electrode force is applied to the electrodes and then to the work pieces. This makes good contact surfaces and reduces the contact resistance. The mechanical analysis at the squeezing stage produces information on stress, deformation and contact area variation. Then the interactions between the electrical and thermal fields are solved simultaneously. The thermal history from the electro-thermal analysis will be served as input to the thermo-mechanical analysis, the results on stress, electrode contact properties and deformation will be passed to the electro-thermal analysis as input. The thermal effect generated by the applied electrical energy is then computed again in the electro-thermal analysis. Such process will be repeated and results will be updated at each time increment until the completion of the welding cycle.

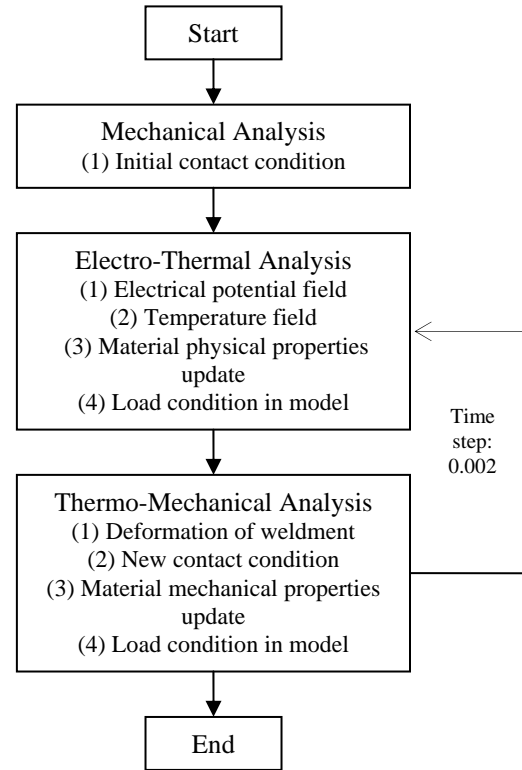


Fig. 1 FEM computational procedure

The model was meshed using three types of elements, as shown in Fig. 2. Plane42 element was used for mechanical analysis (squeeze cycle). In order to simulate the coupled analysis, Plane67 was used. This element has capability of thermal, electrical and thermal-electrical analysis. In structural analysis, this element was replaced with Plane42. There were three contact areas in the model. Two contact areas represented the electrode-sheet interface and the last one represented the sheet-sheet interface. The contact pair elements (Targe169 and Contal71) were employed to simulate the contact areas.

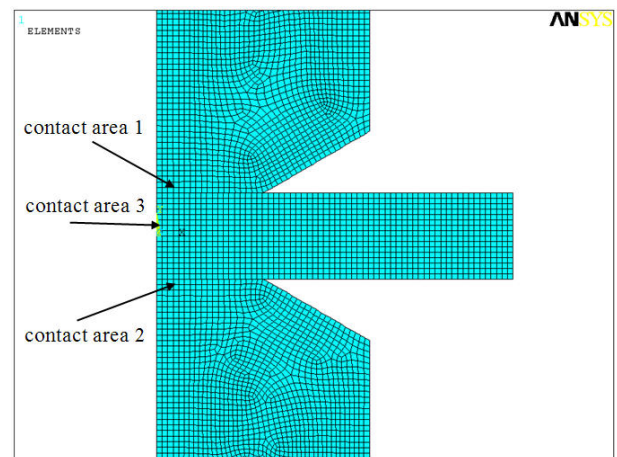


Fig. 2 Mesh generation of model

In this model, the electrode was taken as copper, and

AISI1008 steel sheets were used for the workpieces in the welding process. The properties of these materials including Young Modulus, Poisson ratio, material resistivity, thermal conductivity, specific heat and enthalpy were obtained from reference tables [11]. The boundary conditions for the model, such as air temperature, cooling water temperature, electrode force and applied voltage were also given for the simulations. The characteristics of both the thermal and electrical contact resistance were modeled by using the theoretical analysis as described in the previous section.

Table. 1 shows the characteristics which applied in the simulations. The material properties were considered nonlinear, temperature-dependent. The liquidus temperature of the used material sheet was chosen to be 1527 °C. The welding parameters used in this analysis were: welding current, 50Hz sine wave ac current of 7.5 kA; weld time 11 cycles (0.22s); electrode force, 2kN; hold time, 5 cycles (0.1s). In this research, thermal contact conductivity (TCC) and electrical contact conductivity (ECC) were imposed temperature-dependent at the sheets interface.

Table. 1 Characteristics of simulation

Sheet thickness (mm)	0.8
Electrode face diameter (mm)	5
Ambient air temperature (°C)	25
Temperature of water inside the electrodes (°C)	25
Convection coefficient of ambient air (W/m ² . °C)	21
Convection coefficient of water (W/m ² . °C)	300

IV. RESULTS AND DISCUSSIONS

A. Weldment Displacement

Fig. 3 shows the weldment displacement along X, Y axes. In Fig 3b, the displacement is not symmetric along X axis, because the lower electrode displacement along Y axis was set to be zero. The minimum displacement along X axis is on the edge of electrode at electrode-sheet interface and maximum displacement is on the outer surface of electrode.

Under applied electrode force, measured contact radius at the electrode-sheet interface (E-S), is 2.45mm and at the sheet-sheet interface (S-S), is 3.3mm. Contact radius at E-S was almost equivalent with electrode face radius.

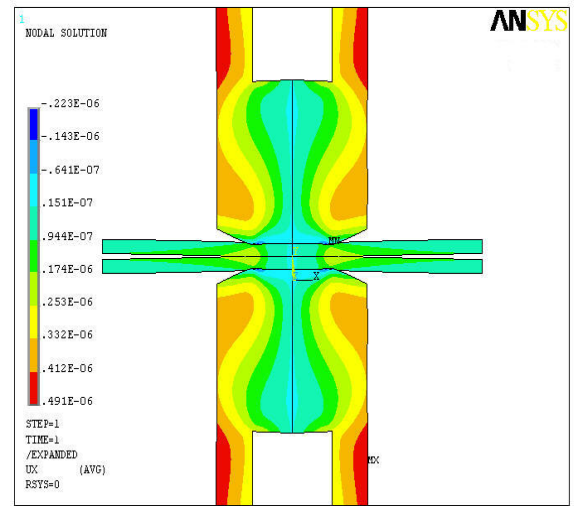


Fig. 3a Displacement of weldment along X axis

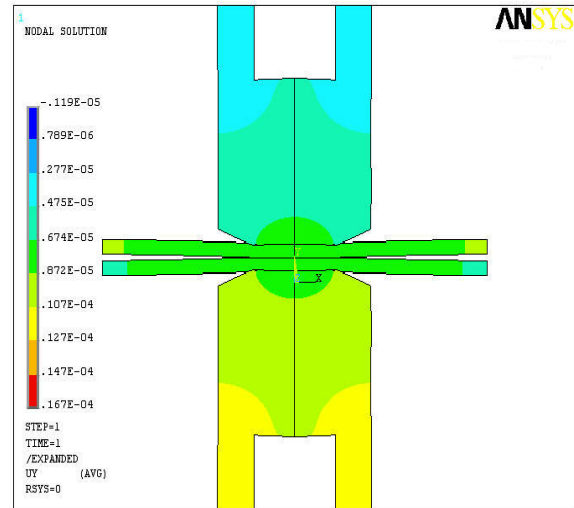


Fig. 3b Displacement of weldment along Y axis

B. Prediction of Nugget Size at Different Welding Stages

Weld nugget is one of the most important parameters of RSW process. Fig. 4 shows temperature distributions of weldment at four different times during the RSW process. The highest temperature was always at the center of faying surface during the whole RSW process. Also temperature of faying surface was more higher than that of electrode-sheet interface.

At the 11th cycle, the highest temperature reached 1536 °C, which means the nugget started to form. The temperature distributions at this time are shown in Fig. 4a. The shape of nugget was a very flat ellipse

As temperature rose, nugget kept growing. Fig. 4b shows temperature distributions at the end of 14th cycle. Maximum temperature at this time was 1876 °C.

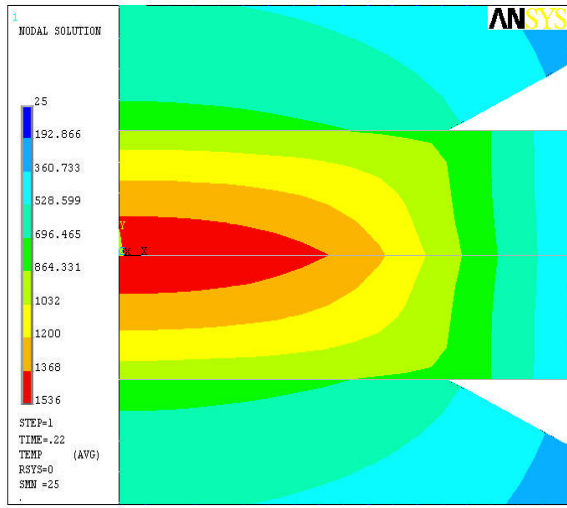


Fig. 4a Temperature distributions at the time of nugget starting to form

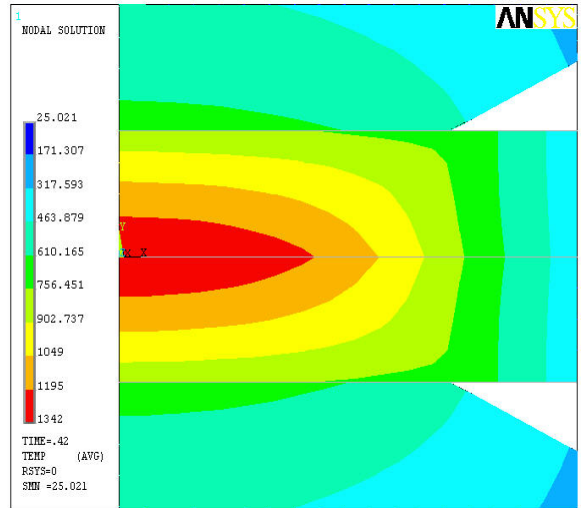


Fig. 4d Temperature distributions at the end of simulation

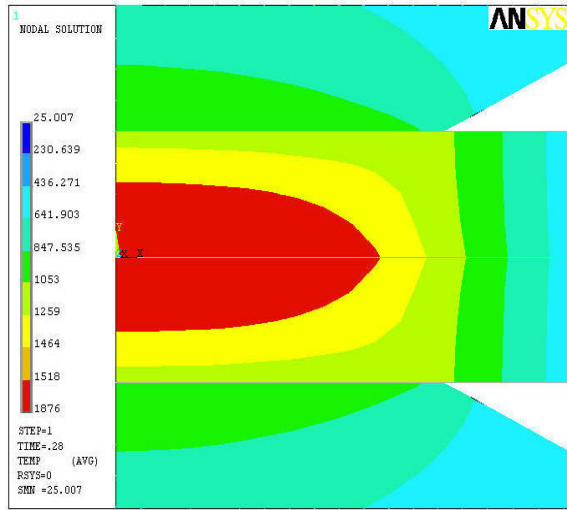


Fig. 4b Temperature distributions at the end of 14th cycle

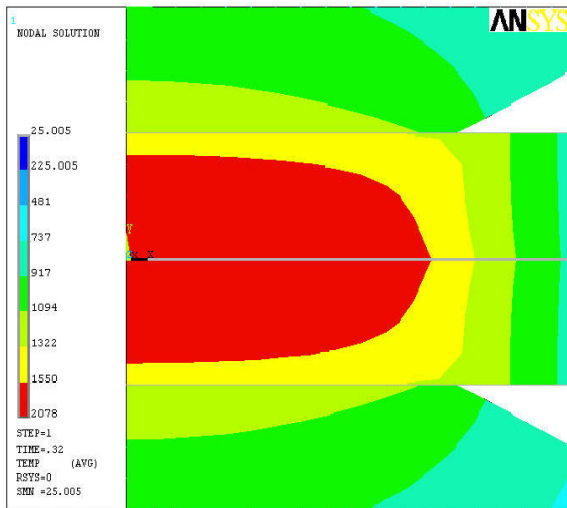


Fig. 4c Temperature distributions at the time of current switching off

The maximum temperature of nugget center (2078 °C) occurred at the end of last ac current cycle, as shown in Fig. 4c. As the electrical current switched off, the weldment started to cool down, So temperature of nugget decreased quickly. At the end of the simulation, temperature of nugget center was 1342 °C (Fig. 4d).

C. Effect of electrode force on nugget size

To study the effect of applied force, first radius of contact area measured. Fig. 5 shows that as electrode force increased, contact radius increased. Due to Joule' heat effect, as contact area enlarged, the generated heat at interfaces reduced and nugget size decreased (Fig. 6). It should be noted that with reduction of force, for increasing nugget size, expulsion phenomena occurs. Therefore, in order to formation of desired weld nugget, selection of suitable force value is important.

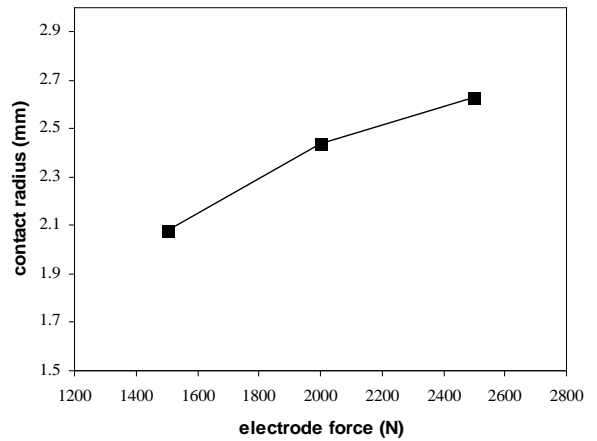


Fig. 5 Effect of electrode force on contact radius

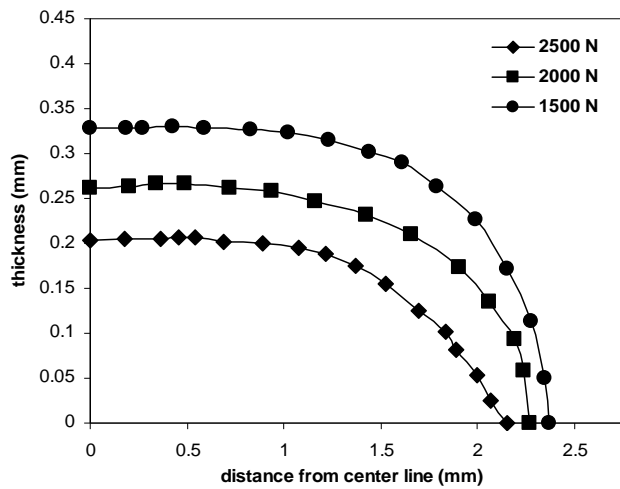


Fig. 6 Effect of electrode force on the size of formed nugget

D. Effect of electrical current on nugget size

According to Joule' heat effect, generated heat due to electrical current is more considerable compared with heat due to time or force parameters. Fig. 7 shows measured nugget size for different applied welding currents. For current 6.5 kA, the formed nugget size was very small. By increase of current to 7.5 kA size of nugget rose remarkably. But rise of nugget size for current 8.5 kA was low.

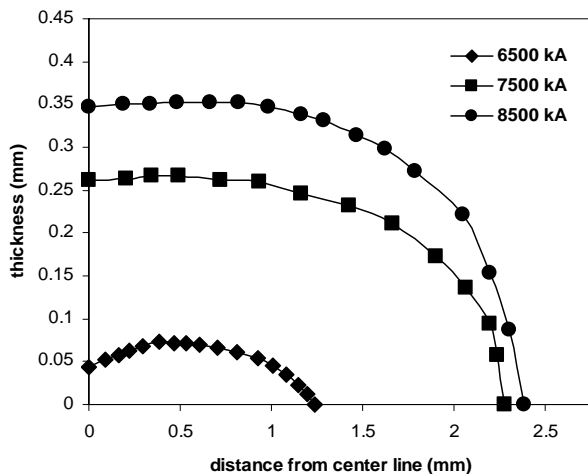


Fig. 7 Effect of electrical current on the size of formed nugget

V. CONCLUSION

In this paper a 2D mathematical model of RSW developed

to predict weld nugget formation through temperature distributions at different welding cycles, and study effect of process parameters on weld nugget size. The results show that:

- 1) As the welding process continues (welding time increases), temperature of sheets interface rises quickly until this area melts and nugget forms. After the formation of nugget, rate of temperature rise is reduces. At the end of welding time, as current switches off, the weldment starts to cool down.
- 2) In a constant welding time, by increase of applied force, nugget size reduces. Because contact area at sheets interface enlarges. This results reduction of current density, which passes through interface and therefore according to Joule' law, lesser heat generates. Thus the time, which temperature of center of faying surface reaches the melting point, rises and less time is left for extension of fusion zone.
- 3) In a constant welding time, increase of welding current is mostly affects on rise of temperature compared with effect of time and force factors. In other words, rate of weld nugget growth is mostly affected by welding current.
- 4) It was concluded that, at low electrode forces and high welding currents, the formed fusion zone is large.

REFERENCES

- [1] O. P. Gupta, and A. De, "An improved numerical modeling for resistance spot welding process and its experimental verification", *Journal of Manufacturing Science*, vol. 120, pp. 246-251, 1998.
- [2] H. S. Cho, and Y. J. Cho, *Welding Journal*, vol. 67, no. 9, pp. 236-244, 1989.
- [3] P. S. Wei, and C.Y. Ho, "Axisymmetric nugget growth during resistance spot welding", *ASME Journal of Heat Transfer*, vol. 112, no. 2, pp. 309-316, 1990.
- [4] J. A. Khan, L. Xu, and Y. J. Chan, "Prediction of nugget development during resistance spot welding using coupled thermal-electric-mechanical model", *Science and Technology in Welding and Joining*, vol. 4, no. 4, pp. 201-207, 1999.
- [5] C. L. Tsai, O. A. Jammal, and J. C. Papritan, "Modeling of the resistance spot welding nugget growth", *Welding Journal*, vol. 71, pp. 47-54, 1992.
- [6] C. L. Tsai, W. L. Dai, D. W. Dickinson, and J.C. Papritan, "Analysis and development of a real-time control methodology in resistance spot welding", *Welding Journal*, vol. 70, no. 12, pp. 339-351, 1991.
- [7] J. A. Khan, L. Xu, Y. J. Chan, and K. Broach, "Numerical simulation of resistance spot welding process", *Numerical Heat Transfer*, vol. 37, Part A, pp. 425-446, 2000.
- [8] A. De, and M. P. Theddeus, "Finite element analysis of resistance spot welding aluminum", *Science and Technology of Welding and Joining*, vol. 7, no. 2, pp. 111-118, 2002.
- [9] E. Klm, and T. W. Eagar, "Transient thermal behavior in resistance spot welding", AWS Detroit Section Sheet Metal Welding Conference III, Southfield, MI, 1988.
- [10] S. P. Timoshenko, and J. N. Goodier, "Theory of Elasticity", 3rd ed., New York: McGraw-Hill, 1970.
- [11] L. O. David, "ASM Handbook", vol. 6, pp. 249-253.